GLOBAL ENGINEERS & TECHNOLOGISTS REVIEW
www.getview.org

NEOTECTONICS OF THE CAUCASUS AND KURA VALLEY, AZERBAIJAN

M. NEMČOK[1], A. A. FEYZULLAYEV[2], F. A. KADIROV[2], G. A. ZEYNALOV[3], R. ALLEN[1], C. CHRISTENSEN[1] and B. WELKER[1]

[1]Energy and Geoscience Institute, University of Utah,
423 Wakara Way, Suite 300,
Salt Lake City, UT 84108, USA,

[2]Institute of Geology, Azerbaijan National Academy of Sciences,
29 A H. Cavid Avenue, AZ1143 Baku, Azerbaijan

[3]Khazar University,
11 Mehseti Street, AZ1096 Baku, Azerbaijan
gzeynalov@khazar.org

ABSTRACT

Analysis of remote sensing, gravity, earthquake, horizontal and vertical motion data in the broader Azerbaijan region, located between the colliding Arabia and Eurasian Platform, indicates the overall dextral transpression. The region undergoes deformation by NW-SE striking transpressional strike-slip faults, pure strike-slip faults and thrusts. It is also deformed by N-S to NE-SW striking sinistral strike-slip faults. The study area is located to the NE of the main indentation point. The direction of indentation is roughly parallel to the NW-SE trending symmetry axis of the fanning horizontal motion vectors, to the NNW-SSE trending axis of the fanning σ_1-stress trajectories and to the fastest slowdown direction of horizontal motions in front of the advancing Arabia, which are all roughly parallel to the Arabian motion vector. The broader Azerbaijan region is situated in the eastern side of these fan-shaped patterns. It is characterized by σ_1 trends progressively changing from NNW-SSE to NE-SW and by the seismoactive zone thickness increasing SE-ward underneath the Kura Valley from 40 to almost 70 km. Its eastern portion, typical by its small-block mosaic structure, contains some unusual local stress regimes. It is argued that they are related to the addition of the regional tectonic stress, highly perturbed along numerous local strike-slip faults, to local stresses generated by interactions of local rotating blocks. This eastern portion is most prone to block rotations, being most distant from the main indentation point and being affected by the least transpressive strike-slip faulting.

Keywords: *Arabia; Eurasian Platform; dextral transpression; stress; strain; indentation*

1.0 INTRODUCTION

The study area, Azerbaijan, is a part of the Alpine-Himalayan orogen. It is formed by the Greater Caucasus Mts., the Lesser Caucasus Mts., the Talysh Mts., the Kura Basin, and the South Caspian Basin (Figure 1). Present-day structures of the study area are controlled by the ongoing collision of the Arabian and African plates with Eurasia (e.g. Philip *et al.*, 1989; Axen *et al.*, 2001; Jackson *et al.*, 2002). The study area is characterized by vertical block movements ranging from –4 to +8 mm/year (Izotov, 1949; Agabekov and Akhmedbeyli, 1958; Sinyagina and Orlenko, 1959; Matskova, 1968; Yashenko, 1977, 1989; Gajiyev and Kadirov, 1980; Lilienberg and Matskova, 1980; Gajiyev *et al.*, 1987). Large magnitude of recent vertical block movements is further highlighted by about 10 km thick Pliocene-Quaternary section in the South Caspian Basin (e.g. Golonka, 2000; Hall and Sturrock, 2000; Guliyev *et al.*, 2001). Block structure of the study area was also interpreted from gravity data (Gajiyev, 1965). Bounding faults were interpreted as deep-seated and located parallel to sharp boundaries or gradients among gravity anomalies. An attempt to tie these interpreted faults with faults mapped on the surface or interpreted from other independent data sets was not made in this study.

The South Caspian Basin is bordered by the Alborz Mountains in the south. The collision-driven deformation in the Alborz Mountains is partitioned into NNE-ward thrusting and NE-SW sinistral strike-slip faulting, both accommodating the Arabian-Eurasian convergence (Allen *et al.*, 2000). Deformation to the west of

the South Caspian Basin in Azerbaijan territory is partitioned into NNE- to NE-ward thrusting and NW-SE dextral strike-slip faulting (Guliyev *et al*., 2002). Start of the Arabian-Eurasian collision dates to Oligocene, based on the occurrence of the shaly Maykop Formation in the broader Greater Caucasus region, the deposition of which is understood as the early collisional consequence (Allen *et al*., 2000). Collision evolved from a subduction, which was parallel neither to the Early-Middle Jurassic rift system nor Late Jurassic-Early Cretaceous sea-floor spreading centers (Dercourt *et al*., 1993). The initial collision closed the Greater Caucasus region, further deformed it together with the Eurasian Platform during Middle-Late Miocene, and the Kura Basin and the Greater Caucasus become zones of the maximum underthrusting (Kopp, 2000). The associated subsidence of the Middle and Lower Kura Basins culminated during Late Pliocene and Quaternary, respectively. Late Pliocene and Quaternary sediments of these basins are as thick as 1-1.2 km and 1.8 km, respectively (Shikhalibeyli, 1996).

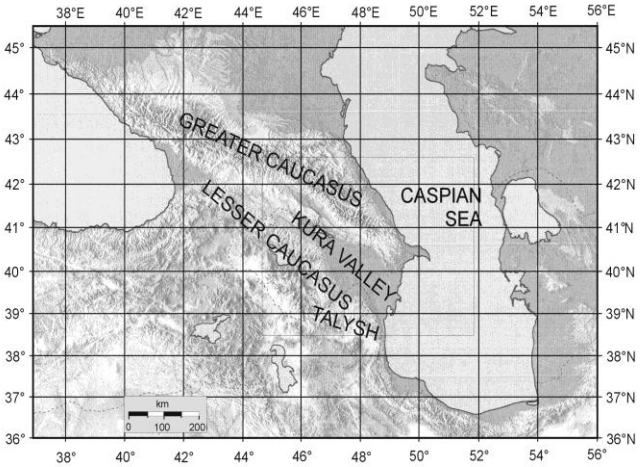

Figure1a: Relief map of the broader Caucasus region

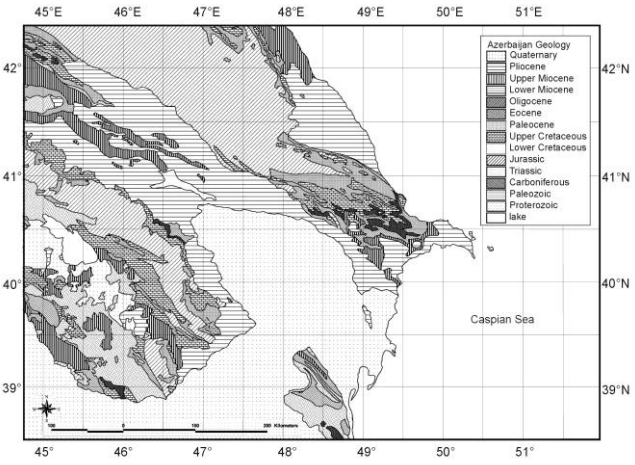

Figure1b: Geologic map of Azerbaijan
(modified from Geological map of Azerbaijan, 1996)

A complex deformation pattern in the broader Caucasus region, including:

(i) the South Caspian subsidence and subsequent folding (Granath and Baganz, 1996);
(ii) a reversal of the dextral strike-slip faulting in the Alborz Mountains to sinistral;
(iii) an eastward lateral extrusion of the central Iran;
(iv) a molasse deposition in the Zagros Mountains;
(v) a reorganization of the Dead Sea transform; and
(vi) a westward escape of the Anatolian blocks

indicates the occurrence of the buoyant Arabian lithosphere in the collision zone (Axen *et al*., 2001). The width of the deformation in the broader Caucasus region, ranging from 500 to 1000 km, is enhanced by the presence of numerous post-Triassic microplates, such as Transcaucasus, Talesh-Alborz, Lut, Farah, Kirsehir, Sakhariya, Central Caspian, South Caspian, Herat, South Pamir and North Pamir (Golonka, 1999, 2000), in the collision zone. All mountain belts surrounding the South Caspian Basin are seismoactive. While no earthquakes deeper than 30 km have been determined in the Kopet Dag, the Alborz Mountains and the Talysh Mountains located along NE, S and W sides of the basin, the earthquakes are as deep as 80 km at the Apsheron-Balkhan sill, which bounds the basin from north (Jackson *et al*., 2002). Despite the complexities due to deformation partitioning into thrusting and strike-slip faulting, dextral and sinistral strike-slip displacements to the north and south of the Kopet Dag and Alborz, respectively, indicate the overall westward movement of the study area in relation to the Arabian and Eurasian plates (Jackson *et al*., 2002). It would be interesting to determine what the proportion of this westward movement in the overall convergence.

The Talysh Mountains and the southwest portion of the South Caspian Basin are characterized by shallow thrust earthquakes (Priestley *et al*.,1994), related to the thrusting of the continental crust of the NW Iran over a remnant oceanic crust of the South Caspian Basin (see Golonka, 2000). It would be interesting to determine what the proportion of this thrusting in the overall oblique convergence.

The thrusting takes part also along both flanks of the Greater Caucasus. Its deformation rate, calculated from the accumulated seismic moment tensor, equals to 1.3 mm/year (Philip *et al*., 1989). Based on the comparison with magnitude of plate movements and offset of linear features, Philip *et al*. (1989) assume that a large part of the deformation is aseismic. It would be interesting to determine how large proportion of this implied aseismic deformation could be explained by strain partitioning.

It is not a goal of this paper to concentrate on a large-scale model of the Arabian-Eurasian collision, which is discussed in detail by numerous studies (e.g. McKenzie 1974; Philip *et al*., 1989; Ruppel and McNutt, 1990; Jackson, 1992; Triep *et al*., 1995; Reilinger *et al*., 1997; Jackson *et al*., 2002). Our goal is to focus on the

© 2011 GETview Limited. All rights reserved

Azerbaijan territory, situated to the north of the NW corner of the Arabian plate, and to study its deformation. In order to do that, remote sensing, earthquake, horizontal motion, gravity and vertical motion data are combined in the ArcView study:

(i) to map geometries of new and pre-existing faults
(ii) to determine displacement sense of these faults, and
(iii) to evaluate the role of these faults in the 500-1000 km wide deformation zone, accommodating the Arabian – Eurasian collision.

2.0 METHODS

Satellite imaging methods used in the paper utilize the Landsat Thematic Mapper (TM) data. Faults were interpreted using indications such as abrupt scarps of the relief, stream offsets, and portions of streams with acute angles or streams flowing against the regional gradient. The TM system has six reflected light channels, including 0.45-0.52, 0.51-0.6, 0.63-0.69, 0.76-0.9, 1.55-1.75, 2.08-2.35 micron bands, and one thermal channel with 10.4-12.5 microns. Images have the resolution of 28.5 m for reflected light channels and 120 m for the thermal band (Prost, 1997; Sabins, 1997). They cover areas 176 x 170 km large. Only 0.45-0.52 micron, 0.51-0.6 micron, and 0.63-0.69 micron bands were used for the interpretation. The interpretation (Figure 2) was made constrained by available geological and geophysical maps. Several interpreted faults were verified in the field.

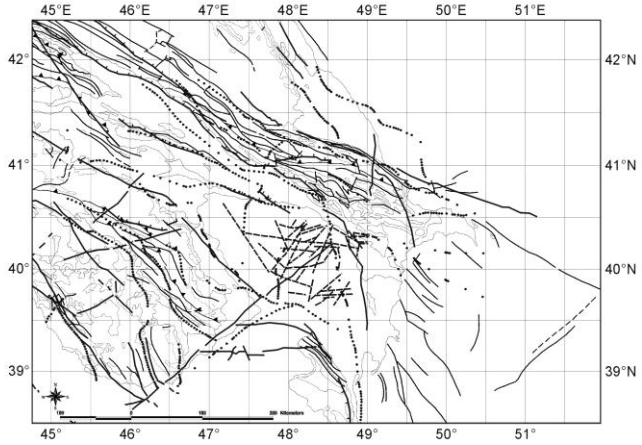

Figure 2: Fault map of the study area

The earthquake data used in the paper (Figure 3) were taken from the earthquake catalogue of the Seismologic Survey of Azerbaijan, made for the time period of 1973-1998, and the IRIS catalogue, made for the time period of 1960-2001. A map with 100 earthquake focal mechanisms shallower than 100 km and having magnitudes greater than 5 (Figure 3a) was made using data from the IRIS database, which compiles published data of Dziewonski *et al*. (1981), Jackson and McKenzie (1998), Shevchenko *et al*., (1999), McClusky *et al*. (2000), Reilinger *et al*. (2000) and Harvard Centroid Moment Tensor (CMT) determinations.

Horizontal motion data based on Global Positioning System (GPS) measurements include data derived from 69 geodetic stations (Figure 4). Most of stations belong to the Caucasian Mountain system that was developed since 1991 on Russian, Armenian and Georgian territories. Fourteen stations belong to the Azerbaijan GPS network developed since 1998 and maintained by both Azerbaijan Academy of Sciences and Massachusetts Institute of Technology. Remaining stations are situated further SW, on the Turkish territory. Measurements used for data in Figure 4 were performed on stations during a period of 1998-2000.

All gravity data used in the paper were taken from the Gravity Map of USSR (1990). These data have a variable grid resolution of 200-1000 by 200-1000 m, with an average of 500 by 500 m. The map of full horizontal gradients (Figure 5) was calculated from the Bouguer anomaly map, derived by first removing the effect of a layer of rock between the measured datum and mean sea level. The density of this layer was 2670 kgm^{-3}. The calculation of full horizontal gradients was then made after assuming that boundaries between various Bouguer anomalies are represented by sub-vertical faults and anomalies represent bodies best described as right-angled parallelepipeds. Full horizontal gradients were calculated by finite-difference method for data points located at junctions of right-angled polygons of the Bouguer anomaly map using the function:

$$G(x,y) = [(\partial g(x,y)/\partial x)^2 + (\partial g(x,y)/\partial y)^2]^{1/2}, \quad (1)$$

© 2011 GETview Limited. All rights reserved

Where :
G(x,y) is the full horizontal gradient,
g(x,y) is the value of the gravity field (sensu Blakely, 1995) and
x, y are Cartesian coordinates.

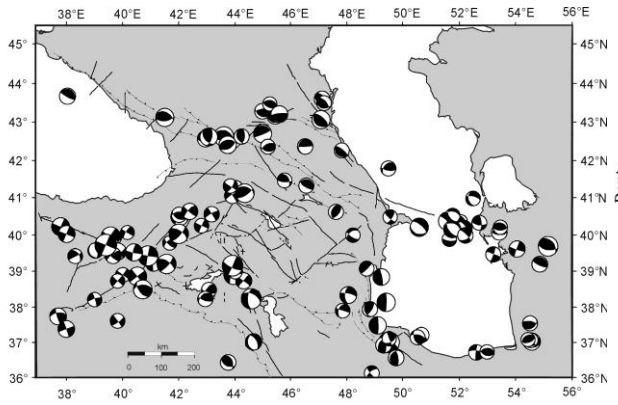

Figure 3a: Earthquake focal mechanism map of the broader Caucasus Region

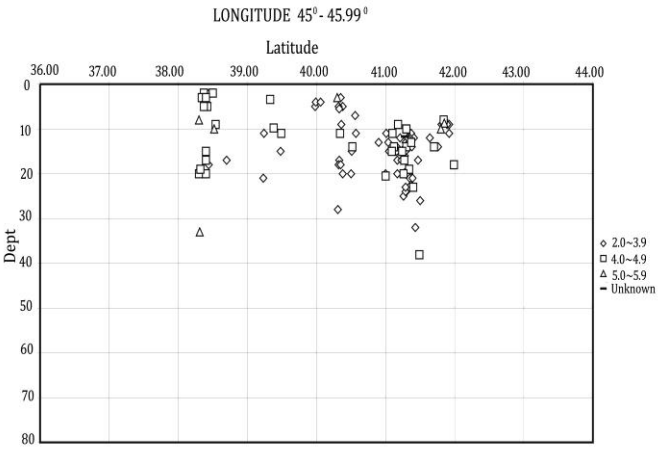

Figure 3b

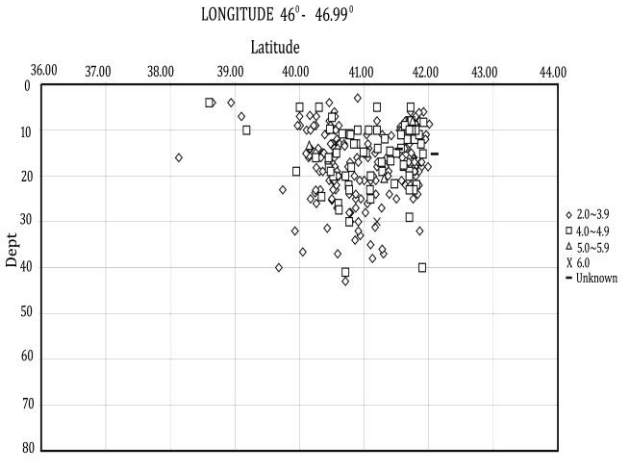

Figure 3c

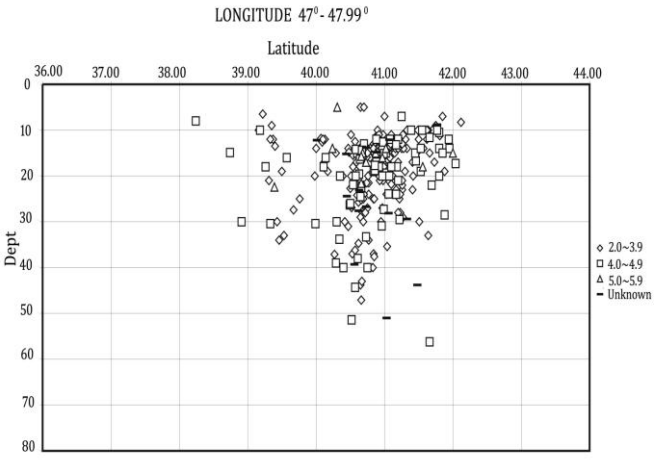

Figure 3d

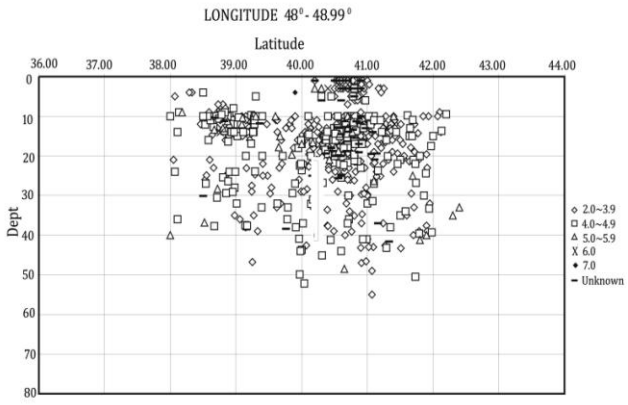

Figure 3e

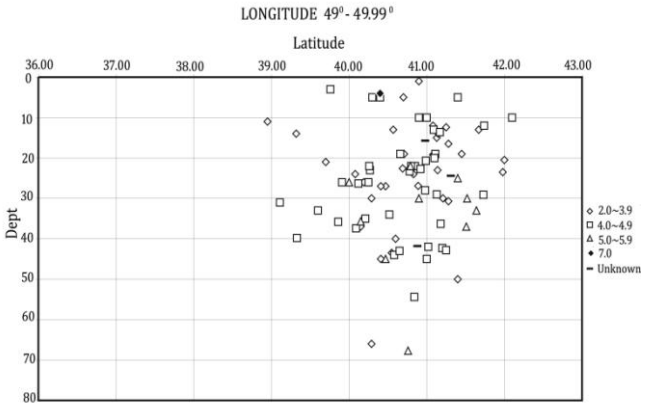

Figure 3f

*** Figure 3b~f**: Depth distribution of earthquake hypocenters (from 1970-1998)

The presence of sub-vertical faults is indicated by full horizontal gradient maxima, as demonstrated in simpler terrains (e.g. Blakely and Simpson, 1986; Edwards *et al.*, 1996; Kadirov, 2000). The calculation of full horizontal gradients was made within a 5 x 5 km grid. The shaded map of full horizontal gradients (Figure 5) uses a 45º- dipping light from 315º (NW).

© 2011 GETview Limited. All rights reserved

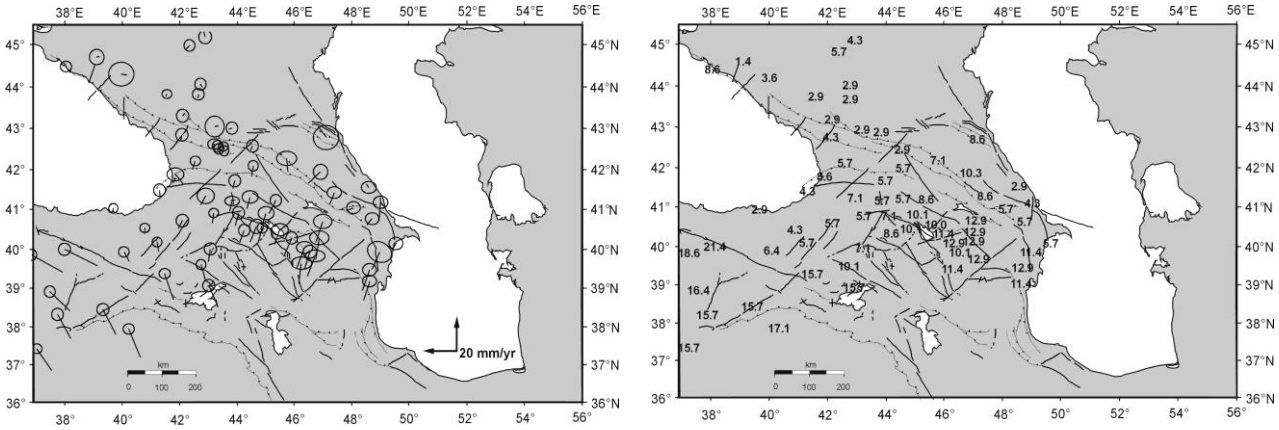

Figure 4: The Map of horizontal motion vectors of the broader Caucasus region (determined by Global Positioning System (GPS) data (Guliyev *et al*., 2002))

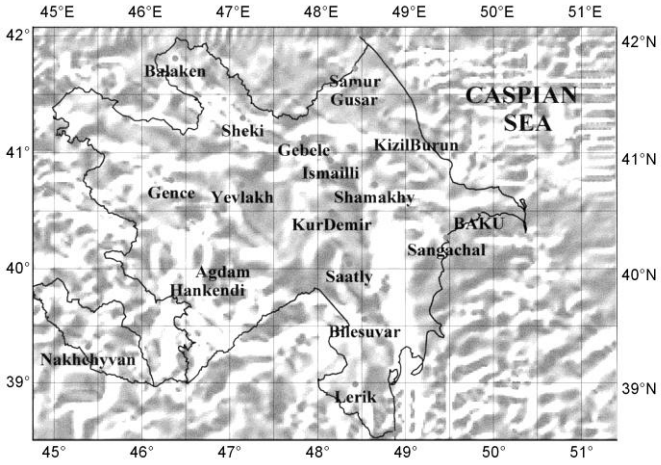

Figure 5: Shaded relief map of the full gradient of the Bouguer gravity field of Azerbaijan. The light vector has an azimuth of 315° and dip of 45°.

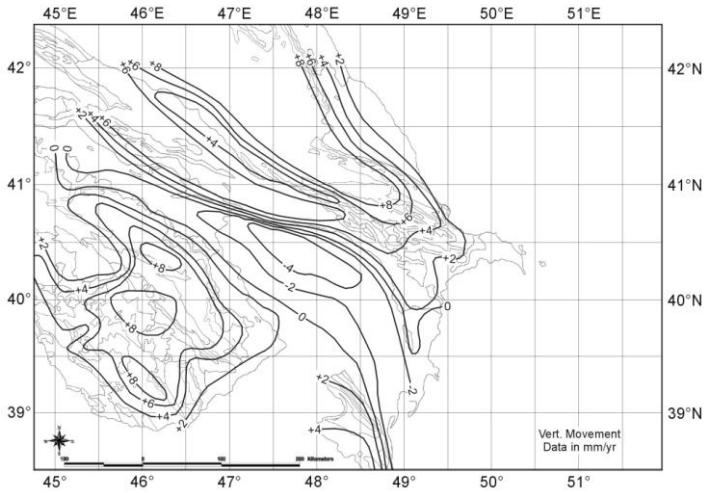

Figure 6: Vertical motion map of Azerbaijan (determined from re-measurements of geodetic polygons). Measurements were made during periods 1949-1953 and 1970-1973 by Lilienberg and Matskova (1980). Contour values are in mm per year. Negative and positive values indicate subsidence and uplift, respectively.

Vertical motion data (Figure 6) were made by repeated re-measurements of geodetic polygons, such as Tbilisi-Baku-Derbent, Nakhchivan-Yevlakh, Nakhchivan-Alat, Alibayramly-Astara, Alibayramly-Bilasuvar-Yevlakh, Yevlakh-Zagatala-Ganja (Izotov, 1949; Sinyagina and Orlenko, 1959; Map of modern vertical movements, 1972; Lilienberg and Matskova, 1980; Yashenko, 1989). Areal extrapolation of vertical motion data was made using morphostructural features of Lilienberg (1980).

Mentioned five data sets were located using the ArcView program, each stored in a separate layer and laid

© 2011 GETview Limited. All rights reserved

over the relief and geologic maps of Azerbaijan and adjacent parts of Armenia, Georgia and Russia (Geological map of Azerbaijan, 1996). Overlapping capability of the ArcView allowed comparisons of faults interpreted from remote sensing and gravity data with faults mapped on the surface onshore or determined from geophysical and well data in the South Caspian Basin (Figure 2). Interpreted faults were compared with horizontal motion data (Figure 4) and earthquake focal mechanisms (Figure 3a), which resulted in determination of fault displacements (Figure 7).

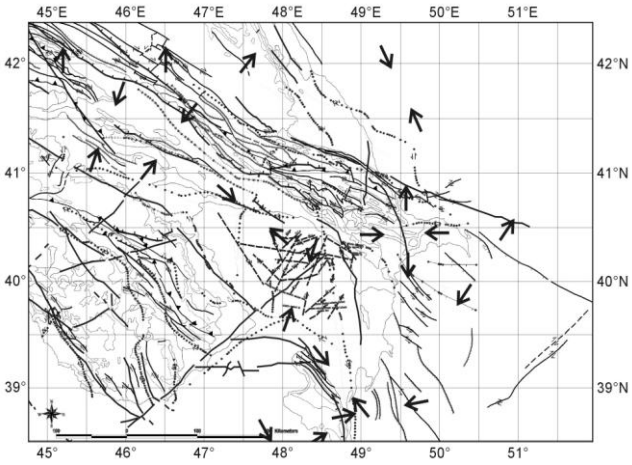

Figure 7a: The Map of fault kinematics (interpreted from fault geometries shown in Figure 2 and principal stresses shown in Figure 3a.) Principal stresses were extrapolated for areas between data points.

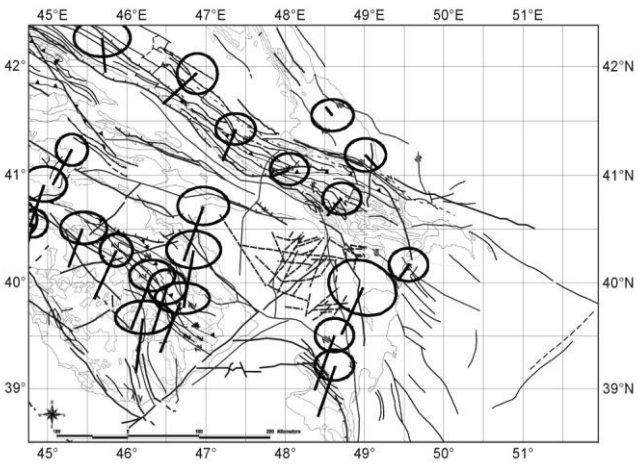

Figure 7b: The Map of fault kinematics (interpreted from fault geometries shown in Figure 2 and horizontal motion vectors shown in Figure 4a.) Determinations were made only for faults close to motion data points.

3.0 DATA

3.1 Faults

Remote sensing data reveal three sets of lineaments, which make up the predominant components of the local structural fabric of the Middle Kura Basin (Figure 2). The first set is formed by NW-SE striking lineaments, making up 10% of the total amount. The second set ranges from WNW-ESE to WSW-ENE striking lineaments, made up by 33.3% of the total lineaments. The third set consists of NNE-SSW to NE-SW striking lineaments, made up by remaining 56.7%. There is a statistical relationship neither between the frequency of occurrence and length of lineaments nor between the strike and length of lineaments.

Figure 2 shows also faults determined by surface geological mapping and those interpreted from earthquake or gravity data. This set of faults demonstrates that the majority is formed by NW-SE striking faults. Mapped faults (Geological map of Azerbaijan, 1996; Shikhalibeyli, 1996; Guliyev *et al*., 2002), based on observation of the dip-slip displacement component, indicate that some NW-SE striking faults comprise reverse and normal faults. Their dip towards NE is prevalent. Mapped NNW-SSE to NE-SW faults in the Greater Caucasus region indicates that they formed as dextral and sinistral strike-slip faults accommodating inhomogeneous shortening.

The Bouguer gravity data (Figure 5) indicate that abrupt boundaries between anomalies, interpreted as deep-seated faults (Figure 2) have also NW-SE strike prevalent, although NNW-SSE to N-S strikes are also present. These faults have the largest density in the Greater Caucasus area. Several of them have been recognized by previous gravity studies and tied to mapped faults, such as the Siyazan, the Caucasian, the Kaynar-Zengi, the Northern Ajinour, the Ajichay-Alat, the Kura, the Lachin-Bashlibel, the Fore-Lesser Caucasian and the Nakhchyvan Faults (e.g. Gajiyev, 1965; Babazadeh, 1995; Shikhalibeyli, 1996). The Bouguer gravity data also indicate a whole number of faults, which were not found by surface mapping in areas lacking marker horizons for their determination.

3.2 Earthquakes

The map of earthquake focal mechanisms determined from earthquakes with magnitudes larger than 5 (Figure 3a) is best described when we divide it into areas comprising the Eurasian Platform, the Greater Caucasus area, the Lesser Caucasus, the area between the Arabian Plate and Black Sea, the Arabian Plate itself together with a narrow zone in front of it, the Talysh Mountains and the broader South Caspian area.

© 2011 GETview Limited. All rights reserved

The Eurasian Platform is characterized by thrust stress regimes that form 75% of its stress solutions. Oblique-slip regimes with reverse component represent 25% of solutions. Trends of the maximum principal compressive stress σ_1 are scattered, ranging from NNW-SSE to NE-SW.

Eighty two percent (82%) of the Greater Caucasus area is controlled by thrust stress regimes. The rest is affected by oblique-slip regimes with transpressional character. Majority of determined σ_1 axes has NE-SW trends. Exceptions, located in central and eastern portions, have ENE-WSW and E-W to ESE-WNW trends, respectively.

Sixteen (16) focal mechanisms resolved for the Lesser Caucasus show its strike-slip character. 19% of solutions have transpressional character. σ_1 directions are quite consistent over the whole area, having NNW-SSE to NNE-SSW trends.

The area between the Arabian Plate and Black Sea is almost exclusively loaded by strike-slip stress regimes with the only one local exception, the thrust solution. σ_1 directions are quite consistent over the whole area, having NNW-SSE to NNE-SSW trends.

The Arabian Plate itself together with a narrow zone in front of it contains strike-slip stress regimes that form as much as 92% of solutions. Remaining 8% is formed by extensional regimes. σ_1 trends here make a converging pattern, consisting of NE-SW trends on its western side, N-S trends in its apex and NW-SE trends on its eastern side. The only exceptions from this pattern are two focal mechanisms on its eastern side, the first one having NE-SW trend and the second one vertical orientation.

The Talysh Mountains are characterized by thrust regimes that make 65% of its control. Remaining stress regimes are represented by transpressional strike-slip regimes. σ_1 directions are extremely scattered, having all possible directions except the N-S one.

The broader South Caspian area is loaded by stresses, the 25% of which comprise strike-slip regimes, 43% thrust regimes and the rest extensional regimes. This region is also characterized by a large scatter of σ_1 directions, although not as large as in the Talysh Mountains. σ_1 axes here are vertical, NE-SW trending, ENE-WSW trending, NW-SE trending and roughly N-S trending.

The earthquake depth distribution made for those with magnitudes larger than 2 shows an interesting pattern. Figures 3b-f documents depth distributions for five 1°-wide longitude stripes between latitudes 36°N and 43°N. Figures 3b-f are arranged to represent stripes progressively more distant from an area of the main indentation. Earthquake depth distributions indicate that the thickness of the seismoactive zone progressively increases in direction away from the main indentation area. The depth of this zone increases from almost 40 km for the 45-46°-longitude stripe, to almost 45 km for the 46-47°-longitude stripe, to 55 km for 47-48° and 48-49° longitude stripes, to almost 70 km for the 49-50°-longitude stripe. The deepest earthquakes along each of these stripes roughly coincide with the surface location of the Kura Valley.

3.3. Horizontal motions

The map of horizontal motion vectors (Figure 4) is best described when we divide it into three regions, including the Arabian indenter, the Eurasian Platform and the 500-1000 km – wide deformation zone between them. Neither Arabia nor the Eurasian Platform is well covered by data. Already the first inspection of the Figure 4 reveals that motion vector patterns from the deformation zone between the main converging plates are much more homogeneous than principal stress patterns from Figure 3a. The reason is a much narrower time span of their collection.

The tip of the Arabian indenter moves to the NE at a pace of 15.7-17.1 mm/year. There are even faster motions recorded in front of it. They are determined in the easternmost portion of the Anatolian wedge, which starts right in front of tip of the indenter and widens westwards, bounded by the North and East Anatolian strike-slip fault zones (Figure 4). The Anatolian wedge moves westward at a rate of 15.7-21.4 mm/year. Motion vectors inside of it change from NW-SE in its southernmost portion to WNW-ESE in its northernmost portion.

The Eurasian Platform is characterized by a large scatter of horizontal motion vectors. They cover practically all possible vergencies; WSW-vergent, W-vergent, NW-vergent, NE-vergent, ENE-vergent, SE-vergent, SSE-vergent and SW-vergent. Motion rates range from 1.4 to 10.3 mm/year.

The 500-1000 km – wide deformation zone between the Arabian indenter and the Eurasian Platform indicates an overall fan pattern of horizontal motion vectors. The axis of its symmetry is a NW-SE trending line that runs from the tip of the Arabian indenter towards Black Sea, through the easternmost tip of the Anatolian wedge. Horizontal motion trajectories to the west of this axis deflect in the counter-clockwise sense from the NW-SE trend to the WNW-ESE trend. The deflection becomes larger with a distance from the indenter. Horizontal motion vectors to the east of this axis deflect in the clockwise sense from the NW-SE trend to the NE-SW trend. The deflection becomes larger with a distance from the indenter. The largest deflection, resulting in the NE-ward motions is recorded along the Greater Caucasus. There is some natural scatter of the horizontal motion pattern but it is not very pronounced.

© 2011 GETview Limited. All rights reserved

Motion rates indicate an overall slowdown from the region adjacent to the Arabian indenter towards the Eurasian Platform, from values of 15.7-21.4 mm/year to values of 2.9-5.7 mm/year.

3.4. Vertical motions

The map of vertical motion vectors (Figure 6) is best described when we divide it into four regions, including the Greater Caucasus, the Kura Valley, the Lesser Caucasus and the Talysh Mountains.

Both Caucasuses have areas affected by uplift faster than 8 mm/year. Maximum velocities recorded here were as high as 10 mm/year. The NW-SE striking uplifting region of the Greater Caucasus has a highly elongate shape. The uplifting region of the Lesser Caucasus has a wide rectangular shape, also with NE-SW strike.

The maximum uplift velocity at the Talysh Mountains reaches 6 mm/year. The data coverage is not good enough to describe the shape of the uplifting region.

The Kura Valley forms a divide between the uplifting Greater Caucasus in the NE from the uplifting Lesser Caucasus - Talysh in the SW. The Kura Valley subsides. The subsidence more-or-less increases in direction away from the main indentation point. The boundary with the uplifting mountains to the SW is rather gradual, while the boundary with the uplifting Greater Caucasus is abrupt.

4.0 INTERPRETATION AND DISCUSSION

4.1 Fault kinematics in the broader Azerbaijan region

A comparison of fault data (Figure 2) with focal mechanism data (Figure 3a) and horizontal motion data (Figure 4) in the ArcView project allows interpreting fault displacements for the broader Azerbaijan region (Figure 7a and 7b, respectively). The interpretation can be best described when we divide the map into areas comprising the Greater Caucasus, the Kura Valley, the Lesser Caucasus, the Talysh Mountains and the South Caspian Basin.

The interpretation shows that the western Greater Caucasus is affected by highly transpressional NW-SE striking dextral strike-slip faults. NW-SE striking faults in the central Greater Caucasus are practically thrusts. NW-SE striking faults in the eastern Greater Caucasus are almost pure dextral strike-slip faults. There are numerous NNW-SSE to NNE-SSW striking lateral ramps in the Greater Caucasus that segment either thrust sheets or blocks among dextral strike-slip faults. They have dextral or sinistral movement sense, according to their geometric relationship to local stress regimes.

The Lesser Caucasus and the Talysh Mountains are dominated by NW-SE striking dextral strike-slip faults. There are also some N-S striking sinistral strike-slip faults present here.

The Kura Valley is deformed by NW-SE striking dextral and NE-SW striking sinistral strike-slip faults dividing it into a mosaic of numerous small blocks. Their average size in the map view is less than 20 by 20 km.

The South Caspian Basin is characterized by NNW-SSE striking dextral strike-slip faults and NW-SE striking normal faults. Highly perturbed local stress regimes control dextral faults of NE-SW strikes in some locations.

Figures 7a and 7b indicate that central and eastern portions of the broader Azerbaijan territory, which is located further away from the main indentation point, are formed by a mosaic of smaller blocks. Some of them are controlled by local stress regimes, which are unusual in comparison to the overall stress regime. They most probably result from complex stress perturbations inside this block mosaic.

4.2. Main indentation point

The dynamic behavior and deformation of the main indentation point of the Arabian indenter are best inferred from Figures 3a, 4a and 4b. The main indentation point is located where the tip of the indenter meets the 500-1000 km wide deformation zone formed between Arabia colliding with the Eurasian Platform. The direction of indentation can be inferred from the NW-SE trending axis of the fan-shaped trajectories of horizontal movements (Figure 4a), NNW-SSE trending axis of the fan-shaped σ_1 trajectories (Figure 3a) or the NW-SE trending direction, running from the Arabian tip towards Black Sea, in which we can see the fastest slowdown of horizontal movements (Figure 4b). Interpreted direction of the indentation is slightly different from earlier northward interpretations (e.g., Shevchenko *et al.*, 1999; Allen *et al.*, 2001) but fully justified by our data shown in Figure 3a, 4a and 4b. The overall fan-shaped arrangement of σ_1 trajectories is similar to several other collisional settings, where data allowed such an interpretation (e.g., Tapponier, 1977; Huchon *et al.*, 1986; Nemčok, 1993).

A closer inspection of the focal mechanism data (Figure 3a) indicates that a narrow zone outside and inside of the Arabian tip is deformed by strike-slip faults, some of them transpressional, which seem to help to focus its indenting to its very tip. This is done by dextral strike-slip faults in the eastern part of this zone and sinistral in its western part, as also observed earlier (e.g., Dercourt *et al.*, 1986; Philip *et al.*,

© 2011 GETview Limited. All rights reserved

1989; see Figure 8). When these dextral and sinistral strike-slip faults curve from their NW-SE and NE-SW strikes, respectively, to roughly W-E strikes at the very tip of the indenter, their displacements change to reverse faulting. Similar changes of the fault character with change of its geometry can be readily found in other curved orogenic belts (e.g., Nemčok *et al*., 1998).

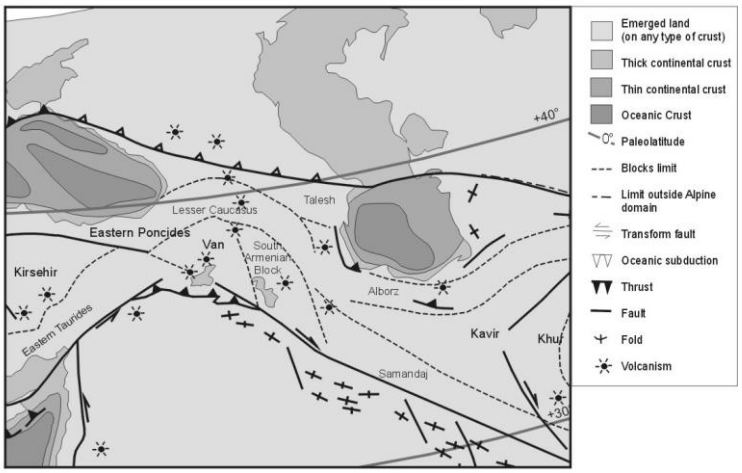

Figure 8: Sketch of the present-day tectonics (modified from Dercourt *et al*., 1986; Philip *et al*., 1989).

4.3. Deformation zone in front of the main indentation point

The collisional zone in front of the Arabian indenter is characterized by different behavior of its portions to the west and east of the main indentation point, in accordance to earlier studies (Dercourt *et al*., 1986; Philip *et al*., 1989). The indentation point forces the collisional zone to be shortened in the direction of indenter's movement. Figures 3a and 4a indicate that axes of both fan-shaped σ_1 trajectories and fan-shaped horizontal movement trajectories are parallel to the Arabian movement vector and originate at the Arabian tip. The fact that the Arabian motion vector is at high angle to the collisional contact between Arabia and the Eurasian Platform (Figure 4a) results in the Anatolian lateral escape between the dextral North Anatolian and sinistral East Anatolian strike-slip faults (e.g., Sengör et al., 1985). Figure 4b shows that Anatolian horizontal movements are faster than movement of the Arabian tip. This is most probably due to the fact that while the Anatolian portion here undergoes a simple shear, the Arabian tip undergoes a strong flattening to become stronger at its tip. The area to the NE of the indentation point is in the region where the material is less prone to the lateral escape, being constrained by the acute angle between the Arabian indenter and the Eurasian Platform (Figure 4a).

Rates of horizontal movements in front of the Arabian indenter show the same scenario (Figure 4b). The fastest slowdown of the horizontal movement inside the collisional zone is along the NW-SW trending line originating at Arabian tip. The region to the NW of the tip experiences the fastest movements, facing a relatively free interface to the west. The area to the NE of the tip experiences a lateral increase of horizontal movements but they are not as fast as those in the NW, because they face constraints resisting the eastward lateral escape.

4.4. Deformation zone further to the NE and E of the main indentation point

As discussed earlier, the stress regime controlling the Anatolian wedge area and the Lesser Caucasus (Figure 3a) has a fan pattern of σ_1 directions which are roughly NNW-SSE trending from the tip of the Arabian indenter towards Black Sea. σ_1 directions deflect toward NW-SE trends to the west of this divide, resembling, for example fanned stress trajectories of the Miocene West Carpathians (Nemčok, 1993). σ_1 trajectories deflect toward NE-SW to the east of this divide, resembling stress trajectories of the Late Paleozoic Welsh Variscides (Gayer *et a*l., 1998). The comparison of σ_1 patterns of the Lesser and Greater Caucasuses indicates that the clockwise deflection of σ_1 trajectories increases as one moves from the indenter toward the contact with the Eurasian Platform. Described fan-shaped σ_1 trajectories somewhat resemble the fan pattern of horizontal motion vectors (Figure 4a) although stress trajectories are more difficult to link because of their large scatter. The main reason for this scatter is that various focal mechanism solutions were determined at different times. Therefore, our data shown in Figure 3a describe stresses relaxed by earthquakes separated by rather long time spans and frequently controlled by locally changed block motions.

σ_1 patterns further to the east of the Greater Caucasus, in the broader South Caspian region, are similar to those of the Greater Caucasus, although showing a large scatter. The σ_1 scatter looks almost random in the southernmost South Caspian Basin and adjacent Talysh Mountains, which are located in

© 2011 GETview Limited. All rights reserved

the region where the distance between the Arabian and Eurasian Plates is largest. However, our observations from Figure 7a described earlier indicate that this is the region with complex stress perturbations, resulting in local anomalously oriented stress regimes, which do not have σ_1 trajectories oriented NNE-SSW to NE-SW according to their position in the overall fan-shape pattern. Some observed local σ_1 directions include trends such as NW-SE, WNW-ESE or ENE-WSW. This is the region that is dissected by systems of NE-SW and NW-SE striking sinistral and dextral strike-slip faults, resulting in a mosaic of relatively small blocks. The overlay of earthquake map (Figure 3a) with fault map (Figure 2) indicates that earthquakes are sometimes located at fault junctions in the region characterized by unusual local stress regimes. Our interpretation of unusual local stress regimes considers mechanisms observed in other complex strike-slip terrains such as Northern Israel or Southern California, characterized by variable rotations of different blocks (e.g. Ron *et al*., 1984; Christie-Blick and Biddle, 1985; Luyendyk *et al*., 1985; Ron and Eyal, 1985). Their block rotations are caused by:

1. rotation among major strike-slip faults and a large number of antithetic shears; or
2. rotation of "randomly" bounded blocks inside a large shear zone (Nelson and Jones, 1987).

Both types of block rotations can develop local areas undergoing extension or compression according to how rotating blocks interact. Such local stress regimes were observed along the Imperial Valley surface rupture in California (Terres and Sylvester, 1981) or near the intersection of the San Andreas and San Jacinto Faults in California (Dibblee, 1977; Nicholson *et al.*, 1986). Based on analogy with mentioned areas, we interpret local unusual stress regimes as caused by the addition of the regional stress, perturbed along numerous strike-slip faults, to local stresses generated by various interactions of local rotating blocks.

The fast deposition along the NW-SE trending Kura Valley (e.g. Shikhalibeyli, 1996) adds an additional complexity to the described block behavior. Kura Valley experiences progressively faster deposition SE-wards. A close inspection of transects in Figure 3b-f reveals a correlation between this trend and the SE-ward thickening trend of the seismoactive zone underneath the valley. This implies that moving away from the main indentation point along the Kura Valley, fault-bounded blocks become potentially thicker and stronger, cooled by the deposition itself, as observed in other areas (e.g. De Bremaeker, 1983; Hutchinson, 1985; Ungerer *et al*., 1990; Jessop and Majorowicz, 1994). The cooling was also observed to be caused by overpressures related to fast deposition, as pointed out in the Kura Valley (Yukler and Erdogan, 1996) or elsewhere (Yalcin *et al*., 1997). Therefore, we interpret local anomalous stresses in the broad region around the Middle and Lower Kura Valley Basin to be related not only to a progressive decrease of the overall transpression eastward as one moves away from the main indentation point, which increases a simple shear component of the overall deformation, but also to progressively stronger blocks eastward, progressively more prone to strike-slip rotation and less prone to pure shear.

This interpretation can be tested by a comparison of horizontal motion rates (Figure 4b) with vertical motion rates (Figure 6) for this area. Without any robust quantification of the strain regime (e.g. Sanderson and Marchini, 1984), we can just qualitatively check, which areas are affected by what proportion of the dextral angular shear versus vertical stretch. We do it by simple assumption that:

1. areas with horizontal movements dominating over vertical ones represent areas affected by simple shear, i.e. prevalent strike-slip regime;
2. areas with vertical movements dominating over horizontal ones represent areas affected by pure shear, i.e. prevalent horizontal shortening; and
3. areas characterized by comparable horizontal and vertical movements are affected by transpression.

We would like to stress that this simple-minded approach is good only for a rough appreciation of general deformation trends, since it fails in understanding strains in detail. It is due to the fact that we do not exactly know mechanisms responsible for vertical and horizontal movements, using our data. While horizontal movements in Figure 4b look reasonable in a comparison with the Arabian-Eurasian convergence rate of 33 mm/year determined by Allen *et al*., (2001), uplift rates of both Caucasuses appear too great to be the result of the plate convergence, indicating enhancement by other mechanisms such as the crustal thickening due to inward lower-crustal flow to beneath both mountain ranges (Mitchell and Westaway, 1999).

Unfortunately, the area covered by vertical motion data is by far not as large as the area covered by horizontal motion data. The horizontal motion data (Figure 4b) indicate an asymmetric bow tie velocity distribution in front of the indenter. Its eastern side has its velocity maximum located in the broad region around the Middle and Lower Kura Valley Basins, the Talysh Mountains and eastern part of the Lesser Caucasus. The highest horizontal motion rates combined with relatively high vertical motion rates overlap with the Talysh Mountains and eastern part of the Lesser Caucasus, indicating transpression. The highest horizontal motion rates combined with low vertical motion rates overlap with the broad region around the Middle and Lower Kura Valley Basins, indicating prevalent strike-slip regime, which would be

© 2011 GETview Limited. All rights reserved

prone to local block rotations. A comparison of Figure 4b with Figure 7a shows that it is exactly this region that is characterized by unusually oriented local stress fields.

5.0 CONCLUSION

1. The study area is deformed by NW-SE striking faults, the kinematics of which varies from area to area, including mostly dextral transpressional strike-slip faults and sometimes thrusts or pure strike-slip faults. N-S to NE-SW striking sinistral strike-slip faults are also present.
2. The direction of the Arabian indentation can be determined as either the NNW-SSE trending axis of the fan-shaped pattern of σ_1 trajectories or the NW-SE trending axis of the fan-shaped pattern of horizontal motion vectors. This axis is a direction of the fastest slowdown of horizontal motions from the Arabian indenter towards the Eurasian Platform. The axis is more-or-less parallel to the Arabian motion vector. Dextral strike-slip faults along the eastern front of the Arabia and sinistral strike-slip faults along the western front seem to help to focus the indentation to the very tip.
3. The western side of the fan-shaped stress pattern is characterized by NNW-SSE trending σ_1 trajectories close to Arabia, which are progressively deflecting to NW-SE trends away from Arabia.
4. The eastern side of the fan-shaped stress pattern is characterized by NNW-SSE trending σ_1 trajectories close to Arabia, which are progressively deflecting to NE-SW trends towards the Eurasian Platform.
5. Portions of the collisional zone are affected by shortening in front of the indenter's tip, by dextral transpression with progressively less amount of perpendicular contraction with the eastward distance from the main indentation point.
6. The broader region around the Middle and Lower Kura Valley Basins, the Talysh Mountains and eastern part of the Lesser Caucasus, located quite far from the main indentation point in the eastward direction, is dissected by NW-SE striking dextral strike-slip faults and NE-SW striking sinistral strike-slip faults into a mosaic of small blocks. Some earthquakes in this region have stress regimes seemingly incompatible with the overall tectonic stress regime. Some of them are located at block junctions. These unusual stresses are caused by addition of the regional stress, perturbed along numerous strike-slip faults, to local stresses generated by interactions of local rotating blocks. These stresses are related to an eastward progressive decrease of the overall transpression, which makes local blocks more prone to rotation.
7. Thickness of the seismoactive zone progressively increases SE-ward underneath the Kura Valley Basin, in accordance with an increasing distance from the main indentation point and increasing depositional rate.

6.0 ACKNOWLEDGEMENT

Described research was funded by Award No. NG2-2283 of the U.S. Civilian Research and Development Fund. Authors are also indebted to Energy and Geoscience Institute for additional support.

REFERENCES

[1] Agabekov, M.G. and Akhmedbeyli, F.S. (1958): Neotectonic Movements in Azerbaijan and Problems Their Study (in Russian). *Geologicheskiy sbornik Lvovskogo Geologicheskogo Obshestva,* Vol. 5 No.6,pp. 13-18.

[2] Allen, M.B., Flecker, R., Bartholomew, I., Ismail-Zadeh, A., Aliyeva, E., Hinds, D. and Simmons, M. (2000): Tectonostratigraphic Evolution of the South Caspian Basin. *AAPG Annual Meetin*g, Expanded Abstracts, AAPG, Tulsa, pp. 5.

[3] Allen, M.B., Inger, S., Blanc, E.J.P., Ghassemi, M., Jackson, J., Talebian, M. and Walker, R. (2001): Neotectonic Orogeny and Basin Development in Iran. *AAPG Annual Meeting*, Expanded Abstracts, AAPG, Tulsa, pp. 5-6.

[4] Axen, G.J., Lam, P.S., Crove, M., Stocki, D.F. and Hassanzadeh, J. (2001): Exhumation of the West-Central Alborz Mountains, Iran, Caspian Subsidence, and Collision-Related Tectonics. *Geology* , Vol.29 No.6,pp.559-562.

[5] Babazadeh, O.B. (1995): Peculiarities of Deep Faults of Azerbaijan on Geophysical Field Anomalies (in Russian). *Proceedings of Geology Institute*, AzNAS, Elm, No 25, pp. 68-90.

[6] Blakely, R.J. (1995): *Potential Theory in Gravity and Magnetic Applications*, Cambridge University Press, New York.

[7] Blakely, R.J. and Simpson, R.W. (1986): Approximating Edges of Source Bodies from Magnetic or Gravity Anomalies. *Geophysics* , Vol.51 No.6,pp.1494-1498.

[8] Christie-Blick, N. and Biddle, K. T. (1985): Deformation and Basin Formation Along Strike-slip Faults. In: Biddle, K.T., Christie-Blick, N. (Eds), *Strike-slip Deformation, Basin Formation, and Sedimentation*. Soc. Econ. Paleont. Mineral. Spec. Publ. 37, pp. 1-34.

[9] De Bremaeker, J.C. (1983): Temperature, Subsidence and Hydrocarbon Maturation in Extensional Basins: A Finite Element Model. *AAPG Bulletin*, Vol.67, pp.1410-1414.

© 2011 GETview Limited. All rights reserved

[10] Dercourt, J.L. and 19 others, 1986. Geological Evolution of the Tethys Belt from Atlantic to the Pamirs since Liassic. *Tectonophysics*, Vol.123 ,pp.241-315.
[11] Dercourt, J., Ricou, L.E. and Vrielynck, B. (Eds.), 1993. *Atlas of Tethys Paleoenvironmental Maps*, Gauthier-Villars, Paris.
[12] Dibblee, T.W., Jr. (1977):. Strike-slip Tectonics of the San Andreas Fault and Its Role in Cenozoic Basin Evolvement. In: Nilsen, T.H. (Ed), *Late Mesozoic and Cenozoic Sedimentation and Tectonics in California*. San Joaquin Geological Society, Bakersfield, pp. 26-38.
[13] Dziewonski, A.M., Chou, T.A. and Woodhouse, J.H. (1981): Determination of Earthquake Source Parameters from Waveform Data for Studies of Global and Regional Seismicity. *Journal of Geophysical Research*, Vol.86, pp.2825-2852.
[14] Edwards, D.J., Lyatsky, H.V. and Brown, R.J. (1996): Interpretation of Gravity and Magnetic Data Using the Horizontal-Gradient Vector Method in the Western Canada Basin. *First Break*, Vol.14 No.6, pp. 231-246.
[15] Gajiyev, R.M. (1965): *Deep Structure of Azerbaijan* (in Russian). Azerneshr, Baku.
[16] Gajiyev, R.N. and Kadirov, F.A. (1980): Periodical Components of Recent Vertical Movements of Southeastern Caucasus (in Russian). *Izvestiya Akademii Nauk Azerbaydjana*, Seriya Nauk o Zemle 3, pp.21-26.
[17] Gajiyev, R.N., Kadirov, F.A., Kadyrov, A.G. and Kunsman, V.V. (1987): The Reveal of Latent Periodicities in Present-Day Vertical Crust Movements Along the Profile Ulan Khol-Baku-Astara (in Russian). *Izvestiya Akademii Nauk Azerbaydjana*, Seriya Nauk o Zemle 1, pp.57-62.
[18] Gayer, R.A., Hathaway, T.M. and Nemčok, M. (1998): Transpressionally Driven Rotation in the External Orogenic Zones of the Western Carpathians and the SW British Variscides. In: Holdsworth, R.E., Strachan, R.A., Dewey J.F. (Eds), *Continental Transpressional and Transtensional Tectonics*. Geological Society, London, Special Publications, No. 135, pp. 253-266.
[19] Geological map of Azerbaijan, 1996. In: Maturin G. Ali-Zadeh A. (Eds), *Reservoir Data, Geochemistry and Seismics of Azerbaijan*. Geological Institute of Azerbaijan National Academy of Sciences and BEICIP-FRANLAB, Baku.
[20] Golonka, J. (1999): Geodynamic Evolution of the South Caspian Basin. *AAPG Bulletin*, Vol.83 No.8,pp.1314.
[21] Golonka, J. (2000): Geodynamic Evolution of the South Caspian. *AAPG International Meeting*, Extended Abstracts, AAPG, Tulsa, pp. 40-45.
[22] Granath, J.W. and Baganz, O.W. (1996): Late Neogene Tectonics of the South Caspian Basin, Azerbaijan. *AAPG Bulletin,* Vol. 81 No.8, pp.1378-1379.
[23] *Gravity Map of USSR*, 1990. Scale 1:2 500 000. Ministry of Geology, Moscow.
[24] Guliyev, I.S., Feyzullayev, A.A. and Tagiyev, M.F. (2001): Source Potential of the Mesozoic-Cenozoic Rocks in the South Caspian Basin and Their Role in Forming the OilAaccumulations in the Lower Pliocene Reservoirs. *Petroleum Geoscience* , Vol.7 No.4, pp.409-417.
[25] Guliyev, I.S., Kadirov, F.A., Reilinger, R.E., Gasanov, R.I. and Mamedov, A.R. (2002): Active Tectonics in Azerbaijan Based on Geodetic, Gravimetric, and Seismic Ddata. *Transactions of the Russian Academy of Sciences*, *Earth Science Section*, Vol. 383 No.2, pp.174-177.
[26] Hall, S.H. and Sturrock, V.J. (2000): The Formation of Supergiants in the Central and South Caspian Basins; Structural Evolution and Plate Tectonic Setting. *AAPG Annual Meeting*, Expanded Abstracts, AAPG, Tulsa, pp. 62.
[27] Huchon, P., Barrier, E., Bremaecker, J.C. and Angelier, J. (1986): Collision and Stress Trajectories in Taiwan: A Finite-Element Model. *Tectonophysics*, Vol.125, pp.179-191.
[28] Hutchinson, I. (1985): The Effects of Sedimentation and Compaction on Oceanic Heat Flow. *Geophysical Journal of the Royal Astronomic Society*, Vol.82, pp.439-459.
[29] Izotov, A.A. (1949): Some Conclusions from Repeatedly Leveling on the WesternCcoastal of Caspian Sea (in Russian). *Proceedings of scientific-technical papers GUGK*, v. XXVII, Moscow, pp. 11-17.
[30] Jackson, J.A. (1992): Partitioning of Strike-slip and Convergent Motion between Eurasia and Arabia in Eastern Turkey and the Caucasus. *Journal of Geophysical Research*, Vol.97, pp.12471-12479.
[31] Jackson, J. and McKenzie, D.P. (1998): A Hectare of Fresh Striations on the Arcitca Fault, Central Greece. *Journal of Structural Geology* , Vol.21 No.1, pp.1-6.
[32] Jackson, J.K., Priestley, M.A. and Berberian, M. (2002). Active Tectonics of the South Caspian Basin. *Geophysical Journal International* , Vol.148, pp.214-245.
[33] Jessop, A.M. and Majorowicz, J.A. (1994): Fluid Flow and Heat Transfer in Sedimentary Basins. In: Parnell, J., (Ed), *Geofluids: Origin, Migration and Evolution of Fluids in Sedimentary Basins*. Geological Society Special Publication 78, pp. 43-54.
[34] Kadirov, F.A. (2000): *Gravity Field and Models of Deep Structure of Azerbaijan*. Nafta-Press, Baku.
[35] Kopp, M.L. (2000): The Recent Deformations of the Scythian and Southern East European Platforms as a Result of Pressure from the Arabian Plate. *Geotectonics,* Vol. 34 No.2, pp.106-120.
[36] Lilienberg, D.A. (1980): Experience of Complex Mapping of Present-day Geodynamics (in example of Azerbaijan) (in Russian). *Present-day motions of Earth crust*. Nauka, Moscow, pp. 65-76.

© 2011 GETview Limited. All rights reserved

[37] Lilienberg, D.A. and Matskova, V.A. (1980): Detail Map of Vertical Movements in Azerbaijan for Periods from 1949-1953 to 1970-1973 years. *Present-day Motions of Earth Crust*. Nauka, Moscow, pp. 68.
[38] Luyendyk, B.P., Kamerling, M.J., Terres, R.R. and Hornafius, J.S. (1985): Simple Shear of Southern California During Neogene Time Suggested by Paleomagnetic Declinations. *Journal of Geophysical Research*, Vol.90, pp.12454-12466.
[39] Matskova, V.A. (1968): Map of Present-day Vertical Motion Velocity in Earth Crust of Caucasus and Southeastern Pre-Azovya (in Russian). *Sb. Sovremenniye dvijeniya Zemnoy Kory* , Vol.3, pp.244-261.
[40] *Map of Modern Vertical Movements of Earth Crust in Eastern Europe*, 1973. Scale 1: 2 500 000, GUGK, Moscow.
[41] McClusky, S. and 28 others (2000): Global Positioning System Constraints on Plate Kinematics and Dynamics in the Eastern Mediterranean and Caucasus. *Journal of Geophysical Research, Vol.105, pp.5695-5719*.
[42] McKenzie, D.P. (1974): Active Tectonics of the Mediterranean Region. *Geophysical Journal of the Royal Astronomical Society*, Vol.30 No.2, pp.109-185.
[43] Mitchell, J. and Westaway, R. (1999): Chronology of Neogene and Quaternary Uplift and Magmatism in the Caucasus: Constraints from K-Ar Dating of Volcanism in Armenia. *Tectonophysics* , Vol.304, pp.157-186.
[44] Nelson, M.R. and Jones, C.H. (1987): Paleomagnetism and Crustal Rotations Along a Shear Zone, Las Vegas Range, Southern Nevada. *Tectonics*, Vol. 6, pp.13-33.
[45] Nemčok, M. (1993): Transition from Convergence to Escape: Field Evidence from the West Carpathians. *Tectonophysics*, Vol. 217, pp.117-142.
[46] Nemčok, M., Houghton, J.J. and Coward, M.P. (1998). Strain Partitioning Along the Western Margin of the Carpathians. *Tectonophysics*, Vol.292, pp.119-143.
[47] *New Catalogue of Strong Earthquakes in USSR Territory from Ancient Period to 1975 year* (in Russian). Nauka, Moscow, 1977.
[48] Nicholson, C., Seeber, L., Williams, P. and Sykes, L.R. (1986): Seismic Evidence for Conjugate Slip and Block Rotation within the San Andreas Fault System, Southern California. *Tectonics*, Vol.5, pp.629-648.
[49] Philip, H., Cisternas, A., Gvishiani, A., Gorshkov, A., (1989): The Caucasus: An Actual Example of the Initial Stages of Continental Collision. *Tectonophysics* , Vol.161, pp.-21.
[50] Priestley, K., Baker, C. and Jackson, J. (1994): Implication of Earthquake Focal Mechanism Data for the Active Tectonics of the South Caspian Basin and Surrounding Regions. *Geophysical Journal International,* Vol. 118, pp.111-141.
[51] Prost, G.L. (1997): *Remote Sensing for Geologists, A Guide to Image Interpretation*, Gordon and Breach Science Publishers, Amsterdam.
[52] Reilinger, R.E., McClusky, S.C., Oral, M.B., King, RW., Toksoz, M.N, Barka, A.A., Kinik, I., Lenk, O. and Sanli, I. (1997): Global Positioning System Measurements of Present-day Crustal Movements in the Arabia-Africa-Eurasia Plate Collision Zone. *Journal of Geophysical Research*, Vol.102, pp.9983-9999.
[53] Reilinger, R.E., Ergintav, S., Burgmann, R., McClusky, S., Lenk, O., Barks, A., Gurkan, O., Hearn, L., Feigl, K., Cakmak, R., Aktug, B., Ozener, H. and Toksoz, N. (2000). Coseismic and Postseismic Fault Slip for the 17 August, M=7.5, Izmit, Turkey Earthquake. *Science*, Vol.89 No.584, pp.1519-1524.
[54] Ron, H. and Eyal, Y. (1985): Interplate Deformation by Block Rotation and Mesostructures Along the Dead Sea Transform, Northern Israel. *Tectonics,* Vol. 4 No.1, pp.85-105.
[55] Ron, H., Freund, R., Garfunkel, Z. and Nur, A. (1984): Block Rotation by Strike-Slip Faulting: Structural and Paleomagnetic Evidence. *Journal of Geophysical Research*, Vol. 89, pp.6256-6270.
[56] Ruppel, C. and McNutt, M. (1990): Regional Compensation of the Greater Caucasus Mountain Based on an Analysis of Bouguer Gravity Data. *Earth and Planetary Science Letters*, Vol.98 No.3-4, pp.360-379.
[57] Sabins, F.F. (1997): *Remote Sensing: Principles and Interpretation*, W.H. Freeman and Company, New York.
[58] Sanderson, D.J., Marchini, W.R.D., 1984. Transpression. Journal of Structural Geology 6, 449-458.
[59] Sengör, A.M.C., Gorur, N. and Saroglu, F. (1985):Strike-Slip Faulting and Related Basin Formation in Zones of Tectonic Escape: Turkey as A Case Study. In: Biddle, K.T. and Christie-Blick (Eds.), *Strike-slip Deformation, Basin Formation, and Sedimentation.* Soc. Econ. Paleont. Mineral. Spec. Publ. Vol. 37, pp. 227-264.
[60] Shevchenko, V.I., Guseva, T.V., Lukk, A.A., Mishin, A.V., Prilepin, M.T., Reilinger, R.E., Hamburger, M.W., Shompler, A.G. and Yunga, S.L. (1999): Recent Geodynamics of the Caucasus Mountains from GPS and Seismological Evidence. *Izvestiya Physics of the Solid Earth*, Vol.35 No.9, pp. 691-704.
[61] Shikhalibeyli, E.S (1996): *Some Problems of Geologic Structure and Tectonics of Azerbaijan* (in Russian). Elm, Baku
[62] Sinyagina, M.N.and Orlenko L.P. (1959): Modern Vertical Movements in Coastal Part of Caspian Sea (in Russian). *Geodeziya i Kartographiya*, Vol. 8, pp. 22-28.
[63] Tapponier, P. (1977): Évolution Tectonique du Systéme Alpin en Méditerranée: Poinconnement et Ěcrasement Rigideplastique. *Bull. Soc. Géol. France*, Vol. 19 No.3, pp.437-460.
[64] Terres, R.R. and Sylvester, A.G. (1981): Kinematic Analysis of Rotated Fractures and Blocks in Simple Shear. *Seismological Society of America Bulletin*, Vol. 71, pp.1593-1605.

© 2011 GETview Limited. All rights reserved

[65] Triep, E.G., Abers, G.A., Lerner-Lam, A.L., Mishatkin, V., Zakarchenko, N. and Starovoit, O. (1995): *Active Thrust Front of the Greater Caucasus, the April 29, 1991, Racha Earthquake Sequence and Its Tectonic Implications*. *Journal of Geophysical Research*, Vol.100 No.3, pp.4011-4033.
[66] Ungerer, P., Burrus, J., Doligez, B., Chenet, P.Y. and Bessis, F. (1990): Basin Evaluation by Integrated Two-Dimensional Modeling of Heat Transfer, Fluid Flow, Hydrocarbon Generation, and Migration. *AAPG Bulletin* 74, pp. 309-335.
[67] Yalcin, M.N., Littke andR., Sachsenhofer, R. F. (1997): Thermal History of Sedimentary Basins. In: Welte, D.H., Horsfeld, B., Baker, D.R. (Eds.), *Petroleum and Basin Evolution. Insights from Petroleum Geochemistry, Geology and Basin Modeling*. Springer, Berlin, pp. 71-167.
[68] Yashenko, V.R. (1977): Present-Day Vertical Movements of Earth Crust Along the Kura River in Azerbaijan (in Russian). *Izvestiya Akademii Nauk Azerbaydjana, Seriya Nauk o Zemle,* Vol. 6, pp.17-22.
[69] Yashenko, V.P (1989). *Geodetic Investigations of The Vertical Movements of Earth Crust* (in Russian). Nedra, Moscow.
[70] Yukler, M. A., Erdogan, T.L. (1996): Effects of Geological Parameters on Temperature Histories of Basins. AAPG Annual Meeting, Abstracts, AAPG, Tulsa, pp. 157-158.

© 2011 GETview Limited. All rights reserved